Available online at www.sciencedirect.com
ScienceDirect
Journal of Nuclear Materials 356 (2006) 122–135
journal of nuclear materials
www.elsevier.com/locate/jnucmat

Retention of hydrogen in fcc metals irradiated at temperatures leading to high densities of bubbles or voids

F.A. Garner [a,*], E.P. Simonen [a], B.M. Oliver [a], L.R. Greenwood [a], M.L. Grossbeck [b], W.G. Wolfer [c], P.M. Scott [d]

[a] *Pacific Northwest National Laboratory, Materials Resources Department, 902 Battelle Boulevard, MSIN: P8-15, Richland, WA 99354, United States*
[b] *Oak Ridge National Laboratory, Oak Ridge, TN 37831, United States*
[c] *Lawrence Livermore National Laboratory, Livermore, CA 94550, United States*
[d] *Framatome, Paris La Defense 92084, France*

Abstract

Large amounts of hydrogen and helium are generated in structural metals in accelerator-driven systems. It is shown that under certain conditions, hydrogen can be stored in irradiated nickel and stainless steels at levels strongly in excess of that predicted by Sieverts' law. These conditions are first, the availability of hydrogen from various radiolytic and environmental sources and second, the formation of radiation-induced cavities to store hydrogen. These cavities can be highly pressurized bubbles or under-pressurized voids, with concurrent helium in the cavities at either low or very high levels. Transmutant sources of hydrogen are often insufficient to pressurize these cavities, and therefore environmental sources are required. The stored hydrogen appears to be stable for many years at room temperature. A conceptual model to describe such behavior requires the continuous generation of hydrogen from (n,p) reactions and possibly other radiolytic sources which can create a supersaturation of hydrogen in the metal, leading to the pressurization of voids and helium bubbles. Once captured in a bubble, the hydrogen is assumed to be in molecular form. Dissolution back into the metal requires chemisorption and dissociation on the bubble surface. Both of these processes have large activation barriers, particularly when oxygen, carbon, and other impurities poison the bubble surface. However, these chemisorbed poisons may reduce but not entirely restrict the ingress or egress of atomic hydrogen.
Published by Elsevier B.V.

1. Introduction

In radiation environments as diverse as those found in accelerator-driven systems, proposed fusion devices and light-water moderated power reactors, the generation rates of helium and hydrogen can be rather large. Accelerator-driven systems (ADS) involving high-energy protons and spallation neutrons have the potential to produce the highest levels of both gases [1]. Whereas most previous attention has been paid to helium generated in structural steels at reactor-relevant temperatures, it

* Corresponding author. Tel.: +1 509 376 4136; fax: +1 509 376 0418.
E-mail address: frank.garner@pnl.gov (F.A. Garner).

0022-3115/$ - see front matter Published by Elsevier B.V.
doi:10.1016/j.jnucmat.2006.05.023

now appears that hydrogen may play an unexpectedly larger role than previously anticipated. Some background needs to be provided concerning the rise of this new perception.

Hydrogen solubility in unirradiated austenitic stainless steels is observed to obey Sieverts' law; which states that the concentration in the metal is proportional to the square root of the local hydrogen overpressure [2]. The concentration in the metal for a given overpressure also increases with increasing temperature in accordance with the Arrhenius equation, with apparent activation energy of around 20 kJ/mol. The concentration in the metal (solubility) can also be affected by the presence of precipitates, dislocations from cold working and by the presence of ferrite. Typically, several 100 appm of hydrogen are observed in fully austenitic 300 series stainless steels after irradiation and equilibration with pressurized water reactor (PWR) and boiling water reactor (BWR) primary coolants [3,4]. Hydrogen is significantly less soluble in ferrite by about an order of magnitude at 300 °C, for example. As shown later, irradiation damage in the form of dislocation loops, network dislocations and especially cavities can have a major impact on the amount of hydrogen found in stainless steels irradiated in light-water reactors (LWRs).

Hydrogen diffusion in unirradiated stainless steels is known to be relatively independent of austenite composition. At typical light-water reactor operating temperatures (280–350 °C), hydrogen is quite mobile in austenite, although very slow relative to ferritic steels [5]. At 300 °C for example, average diffusion distances in austenitic stainless steel are about one millimeter in a day, 4 mm in a month and 15 mm in a year. For ferritic steels, these average diffusion distances can be increased by at least an order of magnitude.

Measurement of hydrogen and its mobility are rather complicated when working with highly radioactive material. Recently, however, it was shown that very accurate measurements of the hydrogen content of highly irradiated steels could be performed on very small amounts (mg) of specimen using a hydrogen analysis system based on thermal desorption and gas mass spectrometry [6]. This technique compliments another existing capability involving very accurate measurements of the helium content using isotopic dilution mass spectrometry on similar small radioactive specimens [7]. In various nuclear environments the cogeneration and potential interaction of these two gases is of current interest, especially with respect to their potential participation in life-limiting phenomena such as void swelling and irradiation-assisted stress corrosion cracking [8].

In a recent paper it was shown that the helium content of a variety of 300 series stainless steels irradiated in a range of nuclear environments could be accurately measured, and also confidently predicted when detailed knowledge was available of the neutron spectra, irradiation history and composition of the steel [3]. The concurrent hydrogen contents, however, could not be predicted as easily, since hydrogen arises in steels from both transmutation and environmental sources, the latter being much harder to characterize. Unlike helium, which is relatively immobile and almost completely retained in the metal, the retention of the very mobile hydrogen is very sensitive to irradiation temperature and damage rate, and particularly to the details of radiation-induced microstructure [1,3,4]. It was possible to show, however, that retained hydrogen levels found in various specimens were usually higher than that generated internally by nuclear (n,p) reactions, leading to the conclusion that environmental sources were also required. It appeared that several 100 appm of additional hydrogen could be stored in microstructural sinks such as black spot damage, dislocation loops and network dislocations.

One particularly interesting and surprising finding of this study was that the retained hydrogen increased very strongly when helium bubbles or vacancy voids began to dominate the microstructure, with the hydrogen retained even after many years of post-irradiation storage [3]. Bubbles and voids are two types of volumetric microstructural defects, often considered as subsets of 'cavities', but each is recognized as having different behavior and different consequences on material performance. Void 'swelling' is a well known, life-limiting phenomenon experienced by essentially all metals and alloys when irradiated at high temperatures by neutrons or charged particles to high levels of atomic displacement [9]. Whereas bubble growth is limited by gas content, swelling is an unsaturable process involving significant increases in component volume and dimensions. Bubbles, however, are also known to serve as precursors to void growth, but have been traditionally thought to contain primarily helium.

In the following sections, the various sources of helium and hydrogen in a variety of fission spectra will be discussed. Then, a number of examples of

apparent hydrogen storage in cavities generated in fission spectra will be presented, followed by cases where such storage did not occur. Details of the various irradiation environments will be provided that may have relevance to the availability of hydrogen sources. After considering the available evidence, the outline of a conceptual model will be presented to describe what conditions favor the long-term retention of hydrogen at larger than expected concentrations in fission spectra and perhaps also in ADS spectra.

2. Sources of helium and hydrogen

In ADS systems there are significant differences in sources of transmutant gases compared to those in fission spectra. In mixed high-energy proton and spallation neutron environments the major alloy components (Fe, Ni, and Cr) all contribute essentially equally to helium and hydrogen generation, primarily through intranuclear cascades involved in spallation reactions. Thus iron-base and nickel-base alloys generate essentially the same gas levels. At the lower neutron energies (<10 MeV) characteristic of various fission-generated spectra, however, the gas sources are much more dependent on alloy composition and neutron spectra [10,11].

Virtually all elements in stainless steel produce helium to some degree during neutron irradiation via (n,α) reactions with neutrons with energies above ~4 MeV. The majority of the helium from such reactions is formed from the five isotopes of natural nickel (primarily ^{58}Ni), with all other major elements typically used in steels having much smaller cross-sections [10]. The recoil range of alpha particles from this type of reaction is rather small, typically less than a micron, leading to minimal energetic losses of helium across the specimen surfaces. Helium ejected from adjacent specimens can also cross into the specimen.

Helium is also formed by interactions with low energy or thermal neutrons that exist at high fluxes in water-moderated reactors. There are two important reactions of this type. The first is the (n,α) reaction with ^{10}B, which comprises 19.9% of natural boron. This contribution to helium production is generally quite small (≪50 appm) and normally saturates quickly with the rapid burnout of this isotope in most reactor neutron spectra having a significant thermal component. Note that ^{6}Li also has a high thermal neutron (n,α) cross-section, but ^{6}Li comprises only ~7% of natural lithium, however, and lithium is generally not a significant impurity in steel.

The second major helium contribution arises from the ^{58}Ni(n,γ) ^{59}Ni(n,α) two-step reaction sequence, which is essentially unsaturable within the range of conditions relevant to LWRs [12]. ^{59}Ni is a radioactive isotope not found in natural nickel. It is important to note that this two-step generation reaction is non-linear with exposure, involving the buildup of ^{59}Ni as the first step. Therefore, this contribution exhibits a delay in its production and continuously accelerates in rate with increasing exposure, only saturating at thermal neutron fluences $>10^{23}$ n/cm^2, well above the range of LWR interest. Most importantly, the degree of acceleration is directly proportional to the thermal-to-fast neutron ratio, which can vary strongly with position both within and outside of LWR cores. The thermal-to-fast ratio increases strongly as the local water to fuel (or metal) ratio increases. Usually there is a strong increase in the ratio just outside the reactor core boundary. Both within and especially outside of LWR cores, this contribution soon becomes the dominant source of helium in nickel-bearing alloys.

Both of these thermal neutron reactions are very exothermic and yield energetic helium atoms with ranges of ~2.5 (boron) and 9.2 (^{59}Ni) μm. Therefore the energetic losses of helium across specimen surfaces are somewhat larger than those arising from high-energy (n,α) reactions. For samples whose minimum dimensions are comparable to the recoil distance, the near-surface regions of specimens must be removed before measurement of helium proceeds. Otherwise, the measurements will be affected by such surface losses.

Hydrogen is also generated by transmutation in fission-generated spectra, but it is important to remember that hydrogen can be introduced into steels by other environmental processes. Examples are corrosion, radiolytic decomposition of water, direct injection from proton recoil following collisions of neutrons with the hydrogen atoms in water, and from equilibrium dissociation and absorption of the hydrogen overpressure maintained in PWR reactors and some BWR reactors. Another example arises from diffusion of transmutant hydrogen produced at large levels in adjacent structural materials or coolants.

In steels, hydrogen arising from transmutation is formed primarily from the various nickel isotopes,

especially ^{58}Ni, interacting with fast neutrons above ~1 MeV [10,11]. The production rate via this reaction is essentially linear with accumulating exposure. Other constituents of typical steels also generate hydrogen by (n,p) reactions, but the cross-sections are much smaller than those of nickel. Due to the lower (n,p) threshold (1 MeV) compared to the ~4 MeV threshold for alpha production, the H/He ratio due to fast neutrons is usually on the order of 14–20, depending on the details of the fast portion of the neutron spectra. However, there is also a ^{58}Ni(n,γ) ^{59}Ni(n,p) reaction, with a thermal cross-section that is about one-sixth of the ^{59}Ni helium production cross-section [13]. The total hydrogen production rate in nickel-bearing alloys is therefore also non-linear with increasing exposure.

Depending on the type of (n,p) reaction the protons are born over a spectrum of energies with maximum energies of several MeV, with maximum ranges of 6–16 μm. Thus energetic losses of hydrogen across surfaces can be significant.

In summary, the major source of helium at high neutron exposure is nickel, and the production rate is proportional to the nickel content and the local thermal-to-fast neutron ratio, but in a non-linear manner with increasing exposure. Transmutant hydrogen is similarly dependent on the nickel content and the thermal-to-fast neutron ratio. The production of helium by boron occurs very quickly, saturating at a rate that is strongly dependent on the thermal neutron flux. Hydrogen, however, can be introduced into irradiated metals by a variety of environmental sources, as will become apparent when considering the experimental examples presented in the following sections.

3. Case #1: Baffle-former bolt from an operating power reactor

The first case involves a 7 cm long, cold-worked 316 baffle-former bolt removed from the Tihange 1 Pressurized Water Reactor in Belgium. The head of the bolt is several mm from the outermost fuel element. The bolt shank is 1.5 cm in diameter and the bolt was embedded in a 304 stainless steel plate with water on both sides. While the threads are in direct contact with the plate, there may be some water in the thin annulus between bolt shank and the plate. The thermal-to-fast neutron ratio varies about a factor of two both along the bolt axis and across the bolt radius. It is important to note that in this type of reactor there is a hydrogen overpressure of 1/3 atmosphere maintained on the coolant.

As shown in Fig. 1, three sections were cut at 1, 25 and 55 mm from the bolt head surface, with doses of 19.5, 12.2 and 7.5 dpa, respectively, as determined by retrospective dosimetry, a technique that determines the neutron exposure from analysis of the activation products in the bolt itself. Additional information on this bolt and its full microstructural and transmutant characterization are presented in other papers [14,15].

The measured helium contents of the three bolt sections ranged from 72 to 49 appm from the 1 to 55 mm positions. These levels are not particularly large and were in good agreement with predictions using the composition of the bolt and the local neutron flux-spectra. The hydrogen measurements at the 1 mm section ranged at 500–700 appm, typical values for neutron irradiated stainless steel in light-water moderated reactors. At the 25 and 55 mm positions in the bolt shank, however, the measurements ranged from 1700 to 3700 appm, even though the neutron exposures were lower than experienced at the 1 mm position. While the differences in temperature at the three positions are not different enough to significantly affect hydrogen retention, the differences are manifested in void formation, a very temperature-sensitive phenomenon, as shown in Fig. 2. It appears that hydrogen may be stored in these cavities, especially at the larger swelling levels formed at slightly higher irradiation temperatures.

Since the thermal-to-fast ratio also varies across the bolt radius, being lower in the center of the shaft, and the bolt surface was in contact with water as a radiolytic source, it could be expected that the hydrogen might also vary across the bolt radius.

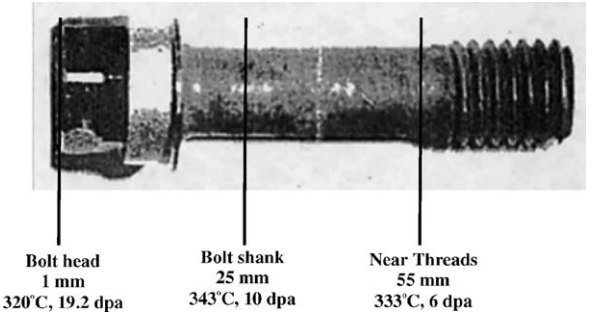

Fig. 1. Location of specimens cut from baffle bolt. The dpa levels have recently been revised to 19.5, 12.2 and 7.5 dpa based on retrospective dosimetry analysis [15].

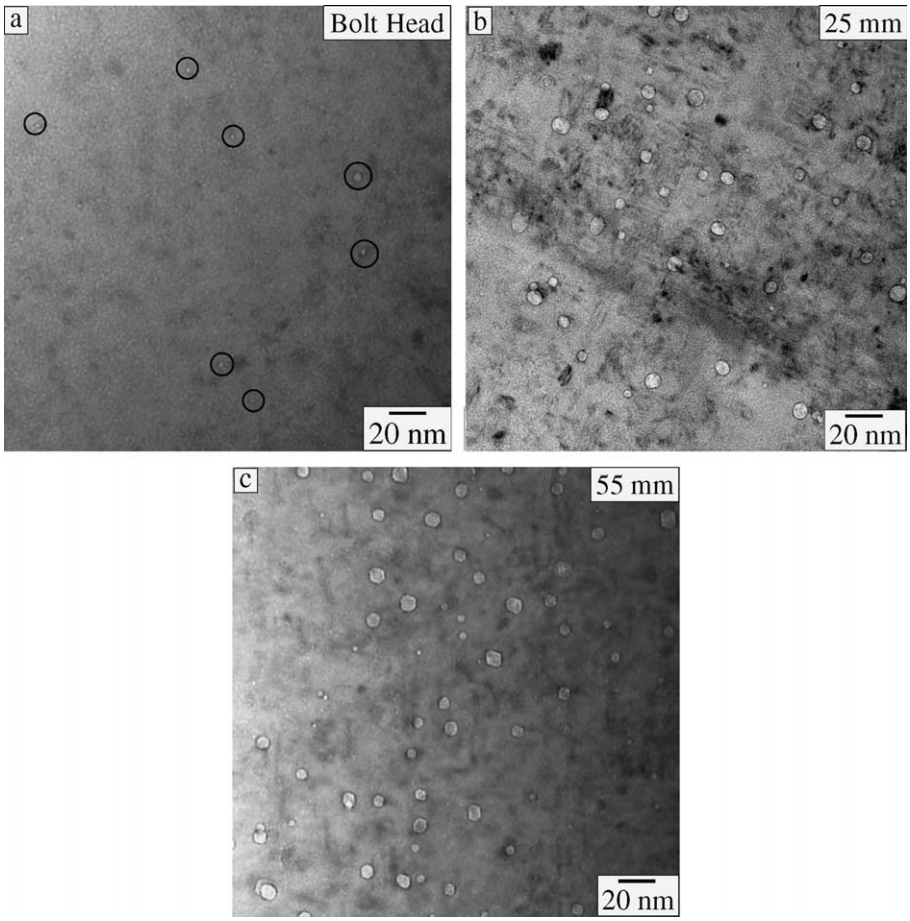

Fig. 2. Cavities observed in the baffle bolt sections [15]. Dotted circles identify some of cavities at the 1 mm position. While the cavities at the 1 mm position are very small (1–2 nm) and cannot be conclusively identified as voids rather than bubbles, the cavities at the other two positions are clearly faceted voids. The mean size of cavities at the 25 and 55 mm positions is ~8 nm. The volumetric swelling at the 1, 25 and 55 mm positions was found to be <0.01%, 0.20% and 0.24%, respectively. As described in [15] the swelling distribution along the bolt is influenced by stress in the bolt shank, and the tendency of the swelling to strongly accelerate as the dpa rate falls.

Unfortunately, no record was maintained of the radial position of the specimens used for hydrogen analysis. Therefore it can not be specified if the 1700–3700 appm hydrogen range observed in the bolt shank specimens represented natural data scatter or additional information on spectral effects on gas production.

4. Case #2: Ti-modified stainless steel in HFIR

Two stainless steel specimens of the US fusion Prime Candidate Alloy (PCA), a modified 316 stainless steel were irradiated in the JP-12 experiment at 400 °C in the high flux isotope reactor (HFIR) in the late 1980s. The specimens were in the form of 3 mm diameter, 0.25 mm thick disks used for electron microscopy. These and similar specimens were stacked in a cylindrical aluminum packet filled with helium gas. This packet was centered in a helium-filled gap, surrounded by an aluminum filler/canister assembly. In the HFIR reactor the gamma flux is very high, leading to 40–50 W/g of heating in stainless steel, depending on the position in the core. The helium gas gap provides thermal isolation to reach the desired temperature in the packet.

The outside of the filler/canister assembly is cooled by water at ~50 °C. In this experiment there was no possibility for the specimens to have direct contact with water. In contrast to the PWR case above, no hydrogen overpressure is maintained on the water coolant in HFIR.

Microscopy results on these specimens were reported by Tanaka, Hamada and co-workers in 1988 and showed the specimens to be densely

packed ($\sim 4 \times 10^{17}$ cm^{-3}) with small (10–20 nm) 'helium-filled cavities' [16,17]. An example of this bubble-like microstructure is shown in Fig. 3, reproduced directly from their paper.

The calculated helium level for these specimens was rather large, 2835 appm at 33 dpa, produced by the very high thermal-to-fast ratio (~2) in this reactor position. Thirteen years later, identical specimens from the same capsule were retrieved from dry storage by the present authors, and measurements were made of the helium and hydrogen. The measured helium levels were 2979 and 3012 appm, within 5% of the calculated values. This agreement provides confidence in our knowledge of the neutron spectrum, and therefore allowed the opportunity to calculate the neutron-induced hydrogen generated, which was predicted to be 884 appm.

Surprisingly, the recently measured hydrogen values were 3864 and 3790 appm, indicating that the hydrogen retained after 13 years storage was more than four times the predicted total generation by transmutation [3]. In effect, these cavities contain as much hydrogen as helium, assuming that both gases are largely contained in the cavities. Examination of all details of the experiment revealed no obvious environmental sources of hydrogen strong enough to account for this 'excess' hydrogen. While this highly voided microstructure has been clearly storing hydrogen for more than a decade, the major hydrogen source is unknown. Therefore, to address the source question in this HFIR experiment, the next experiment was conducted.

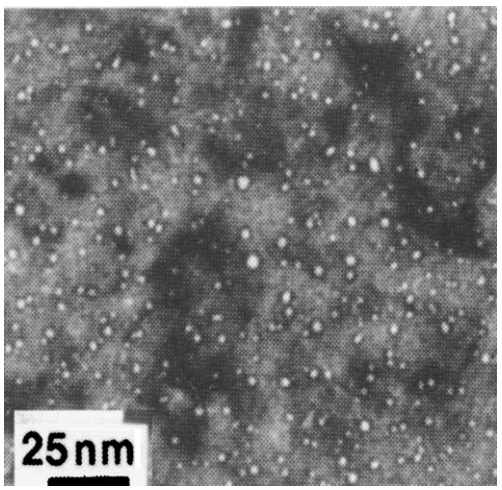

Fig. 3. Bubble-like microstructure observed in HFIR-irradiated USPCA containing $\sim 10^{17}$ cm^{-3} 'helium-filled cavities' after irradiation to 34 dpa at 400 °C by Tanaka et al. [16].

5. Case #3: Pure nickel dosimeters irradiated in HFIR

In the absence of an identifiable environmental source of hydrogen, the possibility of unrecognized transmutant sources was investigated. Perhaps the (n,p) cross-section has been underestimated or perhaps some previously unidentified radioisotope source similar to ^{59}Ni was contributing.

Therefore, it was decided that the short, thin (7 mm × 0.5 mm thick) wire dosimeters of Ni and Fe that were used to determine the spectrum in the JP-12 and follow-on JP-15 experiments should be measured. Since these dosimeter wires were so thin, however, no etching to remove surface material was used. Thus, the measurements will tend to underestimate especially the hydrogen content of the wires, but also of the helium content to a lesser extent [3].

The dosimeters were chosen not only from the 400 °C canister used to irradiate the stainless steel specimens discussed above, but also from the 300, 500 and 600 °C canisters as well, with dpa levels ranging from 34 to 59 dpa. Most of these dosimeters had not been removed from their original sealed aluminum packets, guaranteeing that the wires had not been exposed to moist air or other potential sources of hydrogen over the last decade. On the other hand, the placement of the dosimeters with respect to thermal isolation was not as well controlled as that of the microscopy specimens of Tanaka, and the potential exists that the quoted temperatures may be lower or higher than specified and should therefore be considered only as nominal temperatures.

As will be discussed later, the measurements of the iron dosimeters indicated that iron is not a significant source of the helium or hydrogen, and attention turned to the nickel dosimeters. The hydrogen levels measured for the nickel dosimeters are shown in Fig. 4. In such a comparison, however, it is not possible to judge the original hydrogen content or the amount lost during or after the irradiation. The nickel dosimeters were found to possess very large amounts of hydrogen at levels ranging from 6000 to 16 000 appm, even at *nominal* irradiation temperatures of 600 °C. Most interestingly, the levels were not strongly dependent on irradiation temperature or dpa level. In effect, these

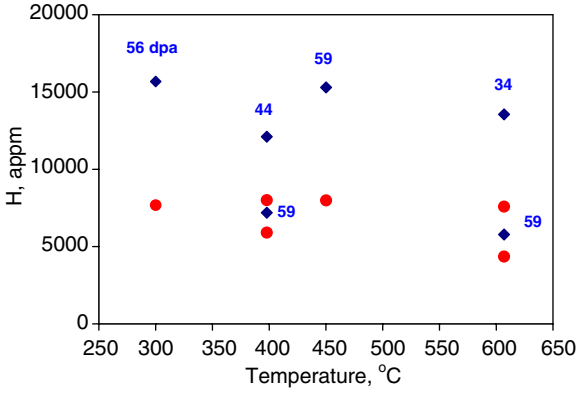

Fig. 4. Hydrogen levels measured in pure nickel dosimeters from the JP-12 and JP-15 experiments in HFIR [3,18]. Blue diamond symbols denote measured values; red circle symbols denote predictions of transmutation-induced hydrogen. The temperatures must be considered as nominal temperatures only. (For interpretation of the references in color in this figure legend, the reader is referred to the web version of this article.)

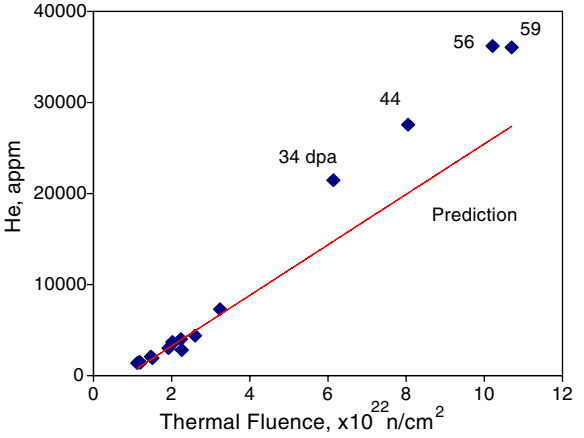

Fig. 5. Comparison of measured helium and predictions as a function of thermal neutron fluence [3,18]. Displacement values are also shown. Data at fluences $<4\times10^{22}$ were measured in an earlier study and used to establish the predictive correlation. These earlier data were derived from larger specimens that were etched to remove surface-affected regions, while for current measurements the thin specimens were not etched and the measured values are therefore underestimates.

specimens *retained* more hydrogen than was calculated to have been formed by transmutation. It must be assumed that energetic and diffusional losses of hydrogen occurred during irradiation and thermal losses afterwards. This implies that the total hydrogen content at the end of the irradiation was probably larger than measured in this experiment.

Since nickel demonstrated such an unexpected response with hydrogen, it was decided to measure the helium content as well, since the predictive correlation was developed from data generated at total thermal neutron exposures that were significantly smaller than those explored in this study. Once again, as shown in Fig. 5, we are surprised to see the unexpected. It appears the measurements are progressively rising with accumulated dpa above the predictive correlation in a manner that is suggestive of another, previously unanticipated, late-term contribution to the helium production. Note that energetic losses of helium have occurred, so the measured numbers are to some extent underestimates.

It was initially suspected that the difference in calculated and measured helium contents might arise from inaccuracies in the cross-sections of the various nickel isotopes. After measuring the ratios of the various nickel isotopes using mass spectroscopy and finding them to be exactly as predicted, this possibility was discounted [18].

It therefore appears that nickel or more appropriately, one of its numerous radioactive daughters and granddaughters may be responsible for both the 'excess' hydrogen and helium. Currently, the most likely candidates are thought to be ^{58}Co and ^{65}Zn, since these isotopes appear to have favorable Q-values for both (n,p) and (n,α) reactions with thermal neutrons. In fact, ^{65}Zn has a very large thermal (n,α) cross-section of 4.7 barns, so it would not be surprising if it also has a large thermal (n,p) cross-section as well [19], although the production of ^{65}Zn is too low to have a major impact on the hydrogen production since multiple steps are required to make this isotope from nickel. Part of the difference may also be explained by increasing the thermal reaction rates for the ^{58}Ni and ^{59}Ni reactions.

While the nickel dosimeter results indicate that some nickel daughter or granddaughter isotope may be providing unexpected contributions to helium and especially hydrogen production, this experiment has not shown clearly that the storage in nickel was actually inside the cavities. The wires were too small to measure swelling and in addition were necessarily destroyed during gas measurement.

However, nickel is well known to exhibit void swelling without significant incubation dose throughout the 300–600 °C range [20,21]. One aspect of swelling in this material is its strong tendency to saturate in swelling at a level that is not only independent of temperature, but also cannot exceed ~8–10% swelling. If hydrogen is stored in cavities, then perhaps the saturation of both hydrogen content and swelling may be directly related.

There is another potential explanation for the dosimeter results, however. If it is allowed that the combined uncertainties in the ^{59}Ni(n,α) and ^{58}Ni cross-sections and thermal neutron fluences can be as large as 20–30% (higher than stated in the literature and thermal neutron measurements) the disparity in helium production might be explained without resort to invoking unidentified transmutant sources. This weakens the argument for an unidentified (n,p) source, however. Finally, this line of reasoning leads us back to the possibility of an environmental source of hydrogen to provide the 'excess'. A detailed analysis of this experiment has recently been published elsewhere [19].

Although the helium and hydrogen contents of the iron dosimeters were also measured, the results will not be reported here, since the iron specimens clearly indicated that helium has been implanted in their surface layers by contact with adjacent nickel specimens. It is therefore assumed that some hydrogen implantation has also occurred, although the hydrogen measurements were in most cases rather low. It can be deduced, however, that nickel and not iron is probably involved in the hydrogen storage in the stainless steel specimens of Tanaka that were discussed in the previous section.

6. Case #4: Stainless steels irradiated in FFTF

Three cold-worked 316 stainless specimens irradiated in the FFTF fast reactor were chosen to see if voids by themselves would store hydrogen when hydrogen was generated primarily by transmutation. These specimens were in contact with the sodium coolant during irradiation. The FFTF core is an oxide-fueled core with rather soft neutron spectra compared to light-water moderated reactors like HFIR or PWR, with mean neutron energy of ~0.5 MeV, and no thermal neutrons. Therefore both the helium and hydrogen generated per dpa in FFTF are significantly less than that generated by LWR spectra.

Two of the specimens had ~8% swelling, as determined by immersion density measurements and confirmed by electron microscopy [22]. One of these was irradiated to 88 dpa at 400–430 °C, and the other to 60 dpa at 550 °C. Although the swelling was approximately the same, the cavity densities were very different, at 2.1×10^{21} and 0.015×10^{21} m^{-3}, respectively and the mean void size was 37 and 190 nm. Thus, the two specimens had very different void surface areas. The third specimen was part of the 400–430 °C irradiation series but was exposed to only 17.5 dpa, producing only 0.28% swelling. The first two specimens had primarily network dislocations and the low exposure specimen had a Frank loop and network structure.

The measured helium contents in the three samples ranged from 5 to 37 appm, in good agreement with predictions. Measured hydrogen levels in the irradiated samples ranged from 322 to 570 appm, indicating that there was no elevated retention of hydrogen as a function of dislocation structure, total void volume or void surface area.

7. Case #5: Model alloys irradiated in FFTF

Four model Fe–15Cr–XNi alloy specimens were irradiated in the fast flux test facility (FFTF) in the ^{59}Ni isotopic tailoring experiment conducted in the below-core region, at damage levels of either 10.2 or 24 dpa [23,24]. The irradiation temperature was 365 °C, which is more prototypic of PWR conditions. Several variables were investigated in this experiment. These were the effect of nickel level (25 and 45 wt%) and the effect of He/dpa ratio. The latter was accomplished by doping one half of the alloys with ^{59}Ni extracted from a nickel-base alloy irradiated in a highly thermalized neutron spectrum. Thus, a side-by-side comparison could be made of the single variable influence of low and high He/dpa rates. The swelling levels were not greatly altered by ^{59}Ni doping, but in general, the swelling was distributed on a much finer scale in the doped alloys. The alloys were swelling in the range of 0.2–0.4% at 10.2 dpa and about several percent at 24 dpa.

At 10.2 dpa the undoped and doped 25 wt% Ni alloys were previously measured to have 7.1 and 165 appm helium, respectively. The 45 wt% Ni alloys had 41.6 and 317 appm at 24 dpa. The measured hydrogen levels in the irradiated samples were rather low, ranging from 184 to 545 appm. It should be noted, however, that several 100 appm would be expected to have been present in the materials prior to irradiation.

In effect, there appears to be no significant storage of excess hydrogen in these FFTF-irradiated specimens, regardless of nickel content, helium level, void surface area or swelling level.

8. Assessment of irradiation data

In the preceding sections, three data sets produced from light-water reactor irradiations clearly

show hydrogen storage at unexpected levels, but the two sets from the FFTF fast reactor do not indicate storage, even for swelling levels of ~8%. What factors may be operating in FFTF to produce this apparently anomalous result?

Several conditions are significantly different in FFTF. First, there are no water-related sources of hydrogen. Second, while the direct transmutation-induced hydrogen source in the steel is lower per dpa compared to the LWR cases, the steel is in direct contact with a large volume of sodium. On first thought, one might assume sodium to be a source of hydrogen, since sodium has a (n,p) cross-section that is about 50% larger than that of iron. However, a comparison of hydrogen solubilities in the above metals reveals that sodium will tend to sequester hydrogen from iron or nickel base metals. If we calculate the relative solubilities of Na, Fe and Ni at 500 °C, then $C(\mathrm{Na})/C(\mathrm{Ni}) = 170$, and $C(\mathrm{Na})/C(\mathrm{gamma\ Fe}) = 320$. Therefore the hydrogen will be predominantly attracted into the sodium, rather than into the steel. Furthermore, the hydrogen content in FFTF sodium is actively maintained at very low levels (~1 appm), well below the solubility limit, being continuously reduced via cold trapping [25].

While the above arguments tend to explain the lack of excess hydrogen storage in FFTF-irradiated specimens, there is another significant difference related to the temperature history upon reactor shutdown. Fast reactors are in general shut down very gradually over a period of 10–20 h in order to reduce thermally induced strains [26]. The temperature therefore falls slowly as the power level is reduced. Even after zero power is reached the sodium temperature never goes below 230 °C in FFTF in order to avoid solidification of the sodium. The specimens may therefore spend two to six weeks at this temperature before being discharged from the reactor. Typical LWRs undergo very different and more abrupt shutdown temperature histories.

If an irradiation flux is a necessary condition for sustaining high levels of hydrogen in metals, some fraction of the hydrogen may be released during the reactor shut down period and more released during subsequent storage at room temperature for extended periods, regardless of whether cavities were present or not. To evaluate the opportunity for hydrogen release after irradiation, the effective diffusion distance of hydrogen was calculated for idealized cooling histories of the various reactor experiments. The effective diffusion distances in the absence of cavities for cooling histories in FFTF, a PWR, and HFIR, as well as during storage are compared in Table 1. These distances are compared to the half thickness of the specific component under study.

For the FFTF case, an exponential cooling history was assumed to estimate the case that most likely would allow hydrogen to be retained, i.e., with the lowest irradiation temperature of 430 °C, instead of the higher 550 °C. The estimated diffusion distance in this case was about five times larger than required for diffusion of hydrogen out from a TEM disc. The result indicates that the measurement of post-irradiation hydrogen content will strongly underestimate the actual concentration maintained during irradiation. A large fraction of any hydrogen accumulated during irradiation will be lost during cooling and in-reactor storage.

In contrast, the PWR cooling history is one that favors retention of hydrogen accumulated during irradiation. The estimated diffusion distance is only about 1/4 of the required distance for escape of hydrogen during cooling. This is a consequence of the lower initial cooling temperature and the larger size of the specimen examined. A linear cooling rate was assumed to overestimate the hydrogen release.

Table 1
Effective diffusion distances during post-irradiation time-at-temperature

Reactor	Cooling condition	Diffusion distance, cm	Required distance, cm	Specimen form
FFTF	Exponential, 0.5 h time constant, 430 °C initial, 320 °C final, 10 h total time	0.07	0.015	TEM disc
PWR	Linear, 343 °C initial, 100 °C final, 1 h total time	0.137	0.647	Bolt embedded in a 304 stainless steel plate
HIFR	Linear, 400 °C initial, 50 °C final, 0.1 h total time	0.0147	0.015+	TEM disc stacked in an Al packet
Storage	Constant 25 °C, 10 years	0.0322	0.015+	TEM disc placed loosely in air-filled container

Actual histories are faster than linear, and therefore it is concluded that the measurement of hydrogen in the PWR specimen is near to the concentration present during irradiation.

The example of HFIR irradiation of stainless steel also was evaluated for a linear cooling rate. Estimated diffusion distances were on the order of the TEM specimen half thickness. For this upper bound estimate, some loss of hydrogen is expected, provided that the lost hydrogen is removed from the environment. The HFIR irradiation occurred in packets that contained mainly Al and there was no intimate path to the outside environment. Because hydrogen is highly insoluble in Al, it is expected that hydrogen is not likely to be released for these marginal diffusion kinetics. At 300 °C the solubility of hydrogen in Al is a factor of 1.2×10^5 lower than for stainless steel.

The effect of extended storage of specimens after irradiation was explored. For storage times of 10 years at 25 °C, significant release of hydrogen is expected. The calculated diffusion distance is about five times that required for release from a TEM disc. For the case of the HFIR packets, other diffusion barriers may exist that may inhibit the ultimate release of hydrogen. The required diffusion distance is marked with the symbol '+' to indicate that release may not be achieved from the irradiation packet simply because the effective diffusion distance is of the order of the TEM disc thickness.

9. Storage capacity in cavities

Calculation of cavity pressures allows estimation of the maximum capacity for storing gases in cavities. The first step normally taken for helium bubbles is to assume equilibrium pressure in the cavities as dictated by the ideal gas law and surface tension with an assumed cavity surface energy of 1 J/m^2. From the measured mean cavity radius and density, the storage capacity was calculated for examples from FFTF, a PWR and HFIR. Table 2 summarizes the storage capacity of measured cavity microstructures compared to measured concentrations of He and H in the irradiated alloys. Cavities in the PWR example appear to be at equilibrium pressure and cavities in HFIR are nearly at equilibrium pressure. In contrast, the observed cavities in FFTF are under-pressurized based on calculations using measured gas concentrations. Because equilibrium pressures can be of the order of thousands of atmospheres, the assumption of ideal gas law behavior needs to be examined, however.

The cavity microstructures have not been measured for irradiation of Ni and Fe in HFIR. Nonetheless, it is possible to estimate storage capacities from assumed swelling values. Fig. 6 shows the calculated storage capacity as a function of cavity size and number density at 400 °C. It is clear that the storage capacity of equilibrium-pressurized cavities is many orders of magnitude larger than is expected from Sieverts' law for absorption of hydrogen in stainless steel. If the swelling is assumed to be 8%, a corresponding size and number density is shown in Fig. 6 and illustrates that quantities on the order of 10 000 appm of molecular hydrogen and helium could easily be stored in a metal. The figure dramatizes the effectiveness of equilibrium-pressurized cavities for storing gas.

9.1. Model requirements based on above observations

It appears that the absence of stored excess hydrogen in the FFTF specimens containing voids is a consequence of the combined influence of the lower generation rate, the higher solubility of hydrogen in sodium compared to that of steel, and to the tendency of hydrogen to diffuse out of steel during a relatively slow descent in power and temperature. However, the PWR bolt case and the two HFIR irradiation cases clearly indicate that hydrogen storage can occur at levels in excess of that predicted by Sieverts' law. Such excess storage

Table 2
Comparison of calculated and measured capacity of cavities for gas storage

Irradiation	Cavity diameter, nm	Cavity, density, number/m^3	Equilibrium cavity storage capacity, molecular ppm	Measured gas conc., molecular ppm	H conc., appm	He conc., appm
FFTF	36.6	2.2×10^{21}	7950	287	500	37
PWR	8.6	0.61×10^{22}	1389	1550	3000	50
HFIR	2.7	4.5×10^{23}	9245	4900	3800	3000

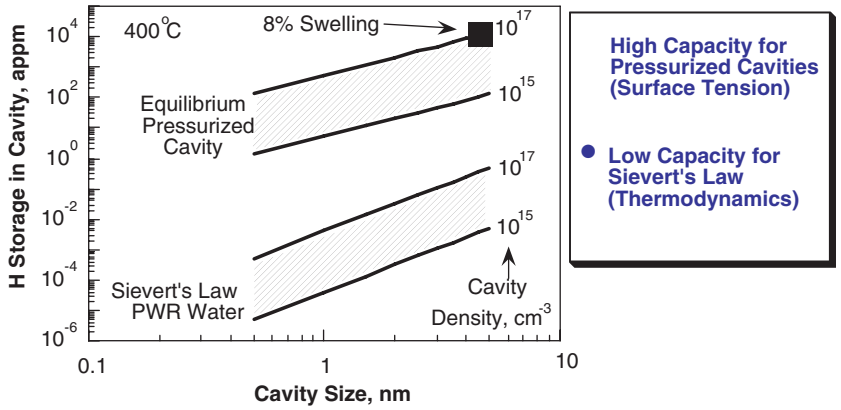

Fig. 6. The storage capacity of cavities is shown as a function of cavity size and number density. The equilibrium pressure assumes a surface energy of 1 J/m^2 and ideal gas law behavior.

occurs when the cavities are clearly under-pressurized or when equilibrium-pressurized, even to very high levels of pressure.

Several questions need to be answered by a hydrogen storage model.

1. What is the form of storage, and is it directly associated with voids?
2. What is the source of the stored hydrogen?
3. Why is the storage so stable at room temperature over long times?

If we assume that the hydrogen is directly stored in the cavities, it is easy to show that such large quantities cannot be in atomic form, adsorbed on the cavity surface. Therefore, the hydrogen in the cavity is most likely in molecular form as H_2. In the PWR bolt and HFIR stainless cases, storage as CH_4 can not be ruled out, but the carbon content of the pure nickel irradiated in HFIR was only 20 appm, probably too low to form the high levels of hydrogen observed.

In the bolt case there are ample sources of hydrogen. In addition to the radiation-induced sources the hydrogen overpressure of 1/3 atmosphere at operating temperature is quite sufficient to provide the large levels of hydrogen required. Andresen demonstrated experimentally this point regarding the permeability of hydrogen in austenitic stainless steels and nickel base alloys in the absence of irradiation damage [27,28]. In PWR primary water in the temperature range 200–360 °C, hydrogen was observed to permeate rapidly through thin wall (0.9 mm) tubes of alloy 600 and achieve steady state permeation rates quickly following changes in hydrogen overpressure. Permeation rates were proportional to the square root of the hydrogen overpressure as expected. Hydrogen dissolved in the water was therefore shown to be the dominant source of hydrogen in PWR primary coolant.

Andresen concluded that general corrosion could not possibly have generated the flux of hydrogen observed. Moreover, it is clear that the oxidized surface on the waterside of the tubes presented no significant barrier to hydrogen adsorption and dissociation into hydrogen atoms that then diffused into the metal, as is well known from studies of high temperature aqueous corrosion of steels.

10. Conceptual model for hydrogen storage and retention

Three fundamental findings can be extracted from the measurements and observations described above:

(1) The amount of hydrogen retained in the irradiated samples is far in excess of the equilibrium solubility as determined by Sieverts' law. Fig. 7 shows the theoretical solubilities at a pressure of 1 bar (0.98 atm) in the temperature range of reactor operation. Even for a PWR with a hydrogen partial pressure of 0.3 atm the equilibrium hydrogen content of stainless steel should be no more than about 20 appm. For HFIR and FFTF, the hydrogen partial pressures were insignificant during reactor operation.

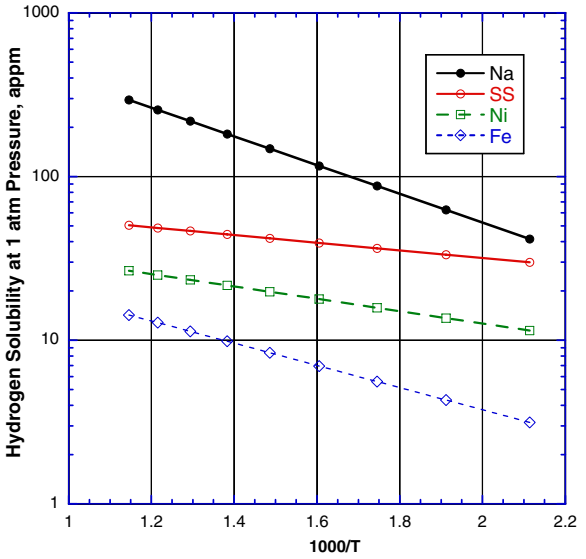

Fig. 7. Equilibrium solubilities of hydrogen in sodium, stainless steel, nickel, and gamma iron [29].

(2) The amount of hydrogen stored and retained in bubbles is also in excess of the cumulative production of hydrogen from (n,p) reactions for the materials irradiated in water-cooled reactors.
(3) For steels irradiated in sodium-cooled reactors, the hydrogen retained is of the order of or less than the cumulative hydrogen generated from nuclear reactions. The coolant sodium sequesters hydrogen from the structural materials as it has a higher solubility as seen from Fig. 7.

The third finding rules out the possibility that the hydrogen could have been introduced during polishing of the samples in preparation for the gas analysis.

One must then conclude that the continuous generation of hydrogen from (n,p) reactions and possibly other radiolytic sources creates in the metal a supersaturation of hydrogen, which leads to the pressurization of voids and helium bubbles. Once captured in a bubble, the hydrogen is in its molecular form. Dissolution back into the metal requires chemisorption and dissociation on the bubble surface. Both of these processes have large activation barriers, particularly when oxygen, carbon, and other impurities poison the bubble surface. However, these chemisorbed poisons do not restrict the ingress or egress of atomic hydrogen.

Since irradiation will produce some radiolytic dissociation of hydrogen in the gas phase, it will provide an alternative pathway for hydrogen in bubbles to re-enter the metal during the reactor operation. A dynamic balance would then be reached between hydrogen absorption from the supersaturated solution in the metal and the radiolysis-induced re-entry.

In water-cooled reactors, an additional source for atomic hydrogen must exist which further raises the supersaturation level of hydrogen in the metal. While the most likely origin of this source is the radiolysis of the coolant water, the results from HFIR irradiations show that the water need not be in direct contact with the supersaturated metal. Just as molecular hydrogen can reform and collect in microscopic bubbles; it must also collect to some degree in gas gaps inside irradiation capsules. Dissociation of molecular hydrogen in these gaps by the neutron and gamma radiation could then feed the supersaturation of samples inside the capsule. Alternatively, other materials such as the aluminum assembly surrounding the internal helium gas gap may provide the necessary hydrogen inside of the irradiation assembly.

Our model remains at the present time qualitative. For a more quantitative model, many kinetic processes must be determined and quantified, including the radiolytic processes in water and in the gaseous mixture of helium and hydrogen inside microscopic bubbles.

It is instructive to estimate the supersaturation of hydrogen in stainless steel that should have existed during HFIR reactor operation. Consider case # 2 described above. The bubble density in the USPCA specimen was 4.5×10^{23} m^{-3} and the average bubble diameter 2.3 nm. Assuming that the resulting bubble volume fraction of 0.29% contained both the measured helium content of about 3000 appm and hydrogen content of about 3800 appm, one finds that 1.7 gas atoms or molecules are stored per vacant atomic site. The helium–hydrogen gas mixture in the bubbles has been compressed to a volume of 4.3 cm^3/mol. According to the high-pressure equations of state [30,31] shown in Fig. 8 for a temperature of 700 K, the gas pressure in the bubble is about 200 kbar or about 20 GPa. In comparison, the surface tension of the small bubbles is about 35 GPa, assuming a surface energy of 2 J/m^2. The gas pressure approaches the value required for bubble growth by dislocation loop punching, as seen in metal tritides [32,33].

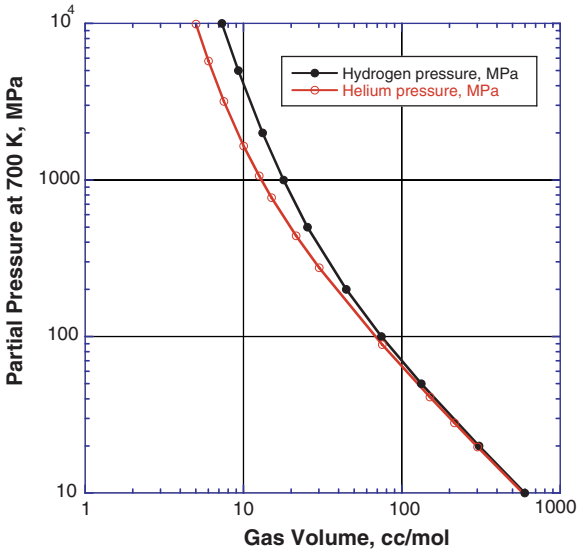

Fig. 8. Pressure of helium and hydrogen at 700 K for high densities.

To maintain hydrogen-containing bubbles under equilibrium conditions at a pressure of 20 GPa at the sample irradiation temperature of 400 °C requires a hydrogen concentration of 1.8 at.% in solution. Clearly, Sieverts' law does not apply in this situation and is of little value to explain the experimental results.

11. Conclusions

It appears that hydrogen gas can be stored in irradiated metals at concentrations significantly in excess of that predicted by Sieverts' law, providing that cavities such as bubbles or voids are formed. The current hypothesis is that hydrogen is stored as H_2 gas in such cavities. In order to explain such storage it is required that supersaturations of atomic hydrogen be maintained in the metals by various transmutation, radiolytic or environmental sources. In general it appears that transmutation sources are insufficient to explain the observed levels of storage.

Acknowledgements

The Offices of Basic Energy Sciences, Fusion Energy, and Nuclear Energy, Science and Technology, US Department of Energy provided support to PNNL for this research under Contract DE-AC06-76RLO 1830. Battelle Memorial Institute operates Pacific Northwest National Laboratory for DOE. The Office of Fusion Energy Science, US Department of Energy, sponsored research at ORNL under contract DE-AC05-00OR22725 with UT-Battelle, LLC. The work at LLNL has been performed under the auspices of the US Department of Energy by the University of California, Lawrence Livermore National Laboratory under contract W-7405-Eng-48.

References

[1] F.A. Garner, B.M. Oliver, L.R. Greenwood, M.R. James, P.D. Ferguson, S.A. Maloy, W.F. Sommer, J. Nucl. Mater. 296 (2001) 66.
[2] W.E. Erwin, J.G. Kerr, WRC Bull. 275 (February) (1982).
[3] F.A. Garner, B.M. Oliver, L.R. Greenwood, D.J. Edwards, S.M. Bruemmer, M.L. Grossbeck, Generation and retention of helium and hydrogen in austenitic steels irradiated in a variety of LWR and test reactor spectral environments, 10th International Conference on Environmental Degradation of Materials in Nuclear Power Systems – Water Reactors, 2001, issued on CD format, no page numbers.
[4] A.J. Jacobs, Hydrogen buildup in irradiated Type-304 stainless steel, Influence of Radiation on Material Properties: 13th International Symposium (Part II), in: F.A. Garner, C.H. Henager Jr., N. Igata (Eds.), ASTM STP 956, 1987, p. 239.
[5] T.P. Peng, C.J. Alstetter, Acta Metall. 34 (1986) 1771.
[6] B.M. Oliver, F.A. Garner, L.R. Greenwood, J. Nucl. Mater. 283–287 (2000) 1006.
[7] H. Farrar, B.M. Oliver, J. Vac. Sci. Technol. A4 (1986) 1740.
[8] F.A. Garner, L.R. Greenwood, Radiat. Eff. Defects Solids 144 (1998) 251.
[9] F.A. Garner, Irradiation performance of cladding and structural steels in liquid metal reactorsMaterials Science and Technology: A Comprehensive Treatment, vol. 10A, VCH Publishers, 1994, p. 419 (Chapter 6).
[10] L.R. Greenwood, J. Nucl. Mater. 216 (1994) 29.
[11] F.A. Garner, L.R. Greenwood, Survey of recent developments concerning the understanding of radiation effects on stainless steels used in the LWR power industry, 10th International Conference on Environmental Degradation of Materials in Nuclear Power Systems – Water Reactors, 2003, p. 887.
[12] L.R. Greenwood, J. Nucl. Mater. 115 (1983) 137.
[13] L.R. Greenwood, F.A. Garner, J. Nucl. Mater. 233–237 (1996) 1530.
[14] D.J. Edwards, F.A. Garner, B.M. Oliver, S.M. Bruemmer, Microstructural evaluation of a cold-worked 316SS baffle bolt irradiated in a commercial PWR, 10th International Conference on Environmental Degradation of Materials in Nuclear Power Systems – Water Reactors, 2001, in CD format, no page numbers.
[15] D.J. Edwards, E.P. Simonen, F.A. Garner, B.M. Oliver, S.M. Bruemmer, J. Nucl. Mater. 317 (2003) 32.
[16] M.P. Tanaka, S. Hamada, A. Hishinuma, P.J. Maziasz, J. Nucl. Mater. 155–157 (1988) 801.
[17] S. Hamada, P.J. Maziasz, M.P. Tanaka, S. Suzuki, A. Hishinuma, J. Nucl. Mater. 155–157 (1988) 838.
[18] D.W. Kneff, L.R. Greenwood, B.M. Oliver, R.P. Skowronski, E.L. Callis, Radiat. Eff. 92&93 (1986) 553.

[19] L.R. Greenwood, F.A. Garner, B.M. Oliver, M.L. Grossbeck, W.G. Wolfer, Surprisingly large generation and retention of helium and hydrogen in pure nickel irradiated at high temperatures and high neutron exposures, Effects of Radiation on Materials, in: M.L. Grossbeck, T.R. Allen, R.G. Lott, A.S. Kumar (Eds.), ASTM STP 1447, ASTM International, West Conshohocken, PA, 2004, p. 529, also in J. ASTM Int. 1(4) (2004), Paper ID JAI11365.
[20] F.A. Garner, J. Nucl. Mater. 205 (1993) 98.
[21] F.A. Garner, Fusion Reactor Materials Semiannual Report for period ending March 31, 1990, DOE/ER-0313/8, p. 125.
[22] G.L. Hankin, Radiation-induced evolution of microstructure and mechanical properties of stainless steels, PhD thesis, Loughborough University, UK, 1999.
[23] F.A. Garner, M.L. Hamilton, L.R. Greenwood, J.F. Stubbins, B.M. Oliver, Isotopic tailoring with ^{59}Ni to study the effect of helium on microstructural evolution and mechanical properties of neutron irradiated Fe–Cr–Ni alloys, in: Proceedings of 16th ASTM International Symposium on Effects of Radiation on Materials, ASTM STP 1175, Denver, CO, June 22–24, 1992, p. 921.
[24] L.R. Greenwood, F.A. Garner, B.M. Oliver, J. Nucl. Mater. 212–215 (1994) 492.
[25] R.A. Bechtold, G.E. Meadows, J.J. McCown, Experience with chemistry monitoring systems at FFTF, in: Proceedings of Third International Conference on Liquid Metal Engineering and Technology, British Nuclear Engineering Society, 1984, p. 39.
[26] F.A. Garner, N. Sekimura, M.L. Grossbeck, A.M. Ermi, J.W. Newkirk, H. Watanabe, M. Kiritani, J. Nucl. Mater. 205 (1993) 206.
[27] P.L. Andresen, T.M. Angeliu, L.M. Young, Effect of martensite and hydrogen on SCC of stainless steels and alloy 600, Paper #01228, Corrosion 2001, NACE.
[28] D.S. Morton, S.A. Attanasio, G.A. Young, P.L. Andresen, T.M. Angeliu, The influence of dissolved hydrogen on nickel alloy SCC: a window to fundamental insight, Paper #01117, Corrosion 2001, NACE.
[29] E. Fromm, E. Gebhardt, Gase und Kohlenstoff in Metallen, Springer-Verlag, Berlin, 1976.
[30] H. Hemmes, A. Driessen, R. Griessen, J. Phys. C: Solid State Phys. 19 (1986) 3571.
[31] W.G. Wolfer, B.B. Glasgow, M.F. Wehner, H. Trinkaus, J. Nucl. Mater. 122&123 (1984) 565.
[32] W.G. Wolfer, Philos. Mag. A 58 (1988) 285.
[33] W.G. Wolfer, Philos. Mag. A 59 (1989) 87.